JOURNAL OF CATALYSIS 108, 24–39 (1987)

Catalysis over Molybdenum Carbides and Nitrides

I. Catalyst Characterization

G. S. RANHOTRA, G. W. HADDIX, A. T. BELL, AND J. A. REIMER

Center for Advanced Materials, Lawrence Berkeley Laboratory, and Department of Chemical Engineering, University of California, Berkeley, California 94720

Received November 13, 1986

The hcp and fcc phases of Mo_2C and the fcc phase of Mo_2N have been prepared and characterized. Mo_2C (hcp) was produced by carburization of metallic Mo. The resulting material is polycrystalline, has a BET surface area of 10–30 m^2/g, and pores 30 Å in diameter. Mo_2N (fcc) is obtained by NH_3 reduction of MoO_3. The nitride has a high degree of crystallinity, a BET surface area of about 180 m^2/g, and pores about 17 Å in diameter. The fcc phase of Mo_2C is produced by exposing Mo_2N to a CH_4/H_2 mixture. This results in a substitution of C for N atoms in the lattice without major changes in the BET area or pore diameter. The preparation of both Mo_2C (hcp) and Mo_2C (fcc) is accompanied by the deposition of free carbon. Selective removal of the free carbon without concurrent removal of lattice carbon cannot be achieved. Air exposure of the carbides does reduce the inventory of free carbon, but at the expense of introducing oxygen into the carbide lattice. The dissolved oxygen cannot be removed by H_2 reduction without removal of lattice carbon. It is possible, though, to remove oxygen from the near-surface region of the carbide particles by pretreating the air-exposed carbide powder in a CH_4/H_2 mixture at 623 K. Use of the carbide and nitride catalysts for CO hydrogenation and C_2H_6 hydrogenolysis causes further changes in the catalyst composition. CO hydrogenation can deposit free carbon and introduces oxygen into the lattice of the catalyst particles. C_2H_6 hydrogenolysis is very efficient in removing oxygen dissolved in the catalyst lattice. © 1987 Academic Press, Inc.

INTRODUCTION

The physical and chemical properties of transition metals are altered significantly by the introduction of carbon or nitrogen into the metal lattice (*1, 2*). The nonmetal atoms enter the voids between the metal atoms and thereby cause an increase in the metal–metal atom distance. One consequence of this is a narrowing of the *d*-band and an increase in the extent of its filling by electrons (*3–5*). These changes modify the adsorptive properties of the metal, as well as its electrical and magnetic properties. Thus, for example, while metallic Mo readily dissociates CO at room temperature, a fully carburized Mo surface will adsorb CO only into a molecular state (*6, 7*). Carburization of Mo and W is also known to temper these metals toward massive dehydrogenation of hydrocarbons (*6*).

An increasing interest has developed in exploring the catalytic properties of transition metal carbides and nitrides. Most of this effort has focused on WC, W_2C, Mo_2C, and Mo_2N but some attention has also been given to TiC and TaC (*8–10*). The reactions studied have included CO hydrogenation (*11–18*), olefin hydrogenation (*19–23*), hydrocarbon reforming (*24–26*), NH_3 synthesis (*13, 27*), CO oxidation (*28*), and NO reduction (*29*). Of particular interest has been the observation that Mo_2C exhibits a CO hydrogenation activity approaching that of Ru and that W_2C exhibits a platinum-like behavior for the isomerization of 2,2-dimethylpropane (*11, 24*). These results demonstrate the potential of transition metal carbides and nitrides to

0021-9517/87 $3.00
Copyright © 1987 by Academic Press, Inc.
All rights of reproduction in any form reserved.

emulate the catalytic properties of noble metals.

In contrast to the level of effort devoted to studies of catalytic activity, much less attention has been given to examining the influence of preparation and pretreatment conditions on composition and structure of transition metal carbides and nitrides. Volpe and Boudart (*30*) have demonstrated recently that high surface area Mo_2N and W_2N powders can be prepared by temperature-programmed reduction of the corresponding oxides with ammonia. Electron diffraction suggests that the conversion of MoO_3 to Mo_2N is topotactic. The final Mo_2N product consists of single crystal platelets containing pores of an average size below 30 Å. Volpe and Boudart (*30*) have also demonstrated that the nitrogen in W_2N and Mo_2N can be substituted by carbon to produce high surface area WC_{1-x} and MoC_{1-x}. The size of the average carbide crystallite was equivalent to that of the nitride, again suggesting a topotactic transformation.

Transition metal carbides are well known to dissolve oxygen (*2*). Since the presence of this element can poison the activity of the carbide for reactions such as ethylene hydrogenation or CO hydrogenation, it is necessary to remove oxygen from the catalyst surface prior to its use (*11, 13, 21–24*). A detailed study of the influence of oxygen on the activity of Mo_2C for ethylene hydrogenation has recently been reported by Leary *et al.* (*31*). They showed that oxygen cannot be removed by thermal activation *in vacuo* or H_2 reduction without also removing a significant amount of bulk carbon.

The purpose of this study was to carry out a detailed examination of Mo_2N and the hcp and fcc modifications of Mo_2C. Particular attention was given to identifying the effects of catalyst preparation and pretreatment on the composition and structure of the catalyst. Attention was also given to establishing the effects of air exposure and the use of the catalysts for CO hydrogenation and C_2H_6 hydrogenolysis. The catalytic properties of the materials examined in this study will be presented separately (*32*).

EXPERIMENTAL

The hcp phase of Mo_2C [hereafter designated Mo_2C (hcp)] was prepared using a modification of the procedure described by Boudart *et al.* (*11*). MoO_3 (Mallinkrodt, 99.5% pure) was reduced to the metal in flowing H_2 [100 cm^3 (STP)/min]. The reduction temperature was slowly increased from 573 K to 973 K over a 5-h period, and then maintained at 973 K for an additional 15 h. The resulting metal was air exposed and crushed prior to converting it to the carbide. The crushed metal was reduced in H_2 at 573 K for 2 h, then heated in a flowing 3/1 : CH_4/H_2 mixture at 573 K for 1 h, then at 673 K for 1 h, and finally at 773 K for 72 h. The flow rate of the CH_4/H_2 mixture was 8 cm^3(STP)/min.

The fcc phases of Mo_2N and Mo_2C [hereafter designated as Mo_2N (fcc) and Mo_2C (fcc)] were prepared following the procedures of Volpe and Boudart (*30*). MoO_3 was first reduced in NH_3 flowing at 135 cm^3 (STP)/min. The reduction temperature was increased from 623 to 723 K over a 3-h period, then from 623 to 973 K over a 2-h period, and finally held at 973 K for an additional 1 h. The Mo_2N (fcc) formed in this manner was cooled to room temperature. To produce the Mo_2C (fcc), Mo_2N (fcc) was carburized in a 1/4 : CH_4/H_2 mixture flowing at 135 cm^3(STP)/min. The carburization temperature was increased linearly from 623 to 973 K over a 10-h period and then maintained at 973 K for an additional 1 h. The samples were then exposed to 1% O_2 in He.

Samples for elemental analysis were submitted in sealed vials to avoid air exposure. The content of C and/or N was determined by combustion of a portion of the sample in the presence of V_2O_5. The amount of Mo was determined by dissolving a second portion of the sample in a mixture of HNO_3

and H_2SO_4 and analyzing the solution by atomic absorption. The oxygen content was obtained by difference. Additional information concerning the contents of C and O in the carbide samples was obtained by temperature-programmed reduction using the apparatus described by Leary *et al.* (*31*).

Structural characterization of the samples was done by X-ray diffraction (XRD) and electron microscopy. XRD measurements were performed with Cu$K\alpha$ radiation on a Siemens Model D500 diffractometer. Electron microscopy was done using a JEOL 200 CX transmission electron microscope operated at 200 kV. In addition to bright-field TEM, electron diffraction patterns were taken for comparison with XRD patterns.

BET and chemisorption measurements were performed using a gas manifold which could be evacuated to 10^{-8} Torr. N_2 isotherms were measured at 78 K and the total surface area was determined by fitting the BET equation to the data. Chemisorption was performed with CO at room temperature. Following the determination of a total CO isotherm, each sample was evacuated for 2 h or more and a second isotherm was measured. The difference between the two isotherms represents the isotherm of CO chemisorbed irreversibly. The amount of CO adsorbed irreversibly was determined by extrapolating the plateau in the isotherm for irreversible adsorption to zero pressure.

To determine the effects of reaction conditions on catalyst composition and structure, samples were placed in a small quartz reactor connected to a gas manifold and a gas chromatograph. The reactor is constructed with two three-way stopcocks so that after reaction, the sample can be isolated and transferred to the chemisorption apparatus without air exposure.

RESULTS

Mo_2C (hcp)

The structure and composition of Mo_2C (hcp) were examined following its synthesis and exposure to air. The XRD pattern for the sample is given in Fig. 1. The peaks marked by ‡ are characteristic of the hcp phase of Mo_2C and the indicated *d*-spacings coincide very well with those reported previously (*33*). The peak designated by † is due to a small amount (13%) of metallic Mo left in the sample. It is significant to note that there is no evidence for bulk MoO_2 or MoO_3.

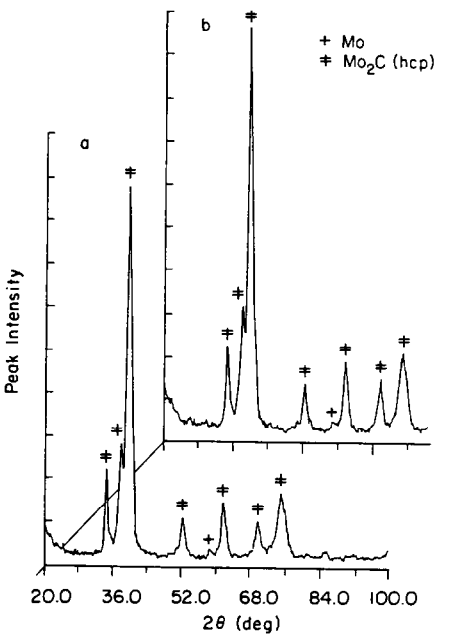

FIG. 1. XRD Patterns of Mo_2C (hcp): (a) following synthesis and air exposure, (b) following CO hydrogenation and air exposure.

TEM micrographs and an electron diffraction pattern of the sample are given in Fig. 2. It is difficult to discern much detail about the structure of the sample since the particles are fairly thick and hence appear nearly opaque. The presence of Moiré fringes in Fig. 2c suggests that the sample is highly polycrystalline, the fringes being due to overlapping microcrystallites rotated relative to each other (*34*). The polycrystalline nature of the sample is also supported by the electron diffraction pattern which shows rings rather than distinct spots. The *d*-spacings determined from the electron

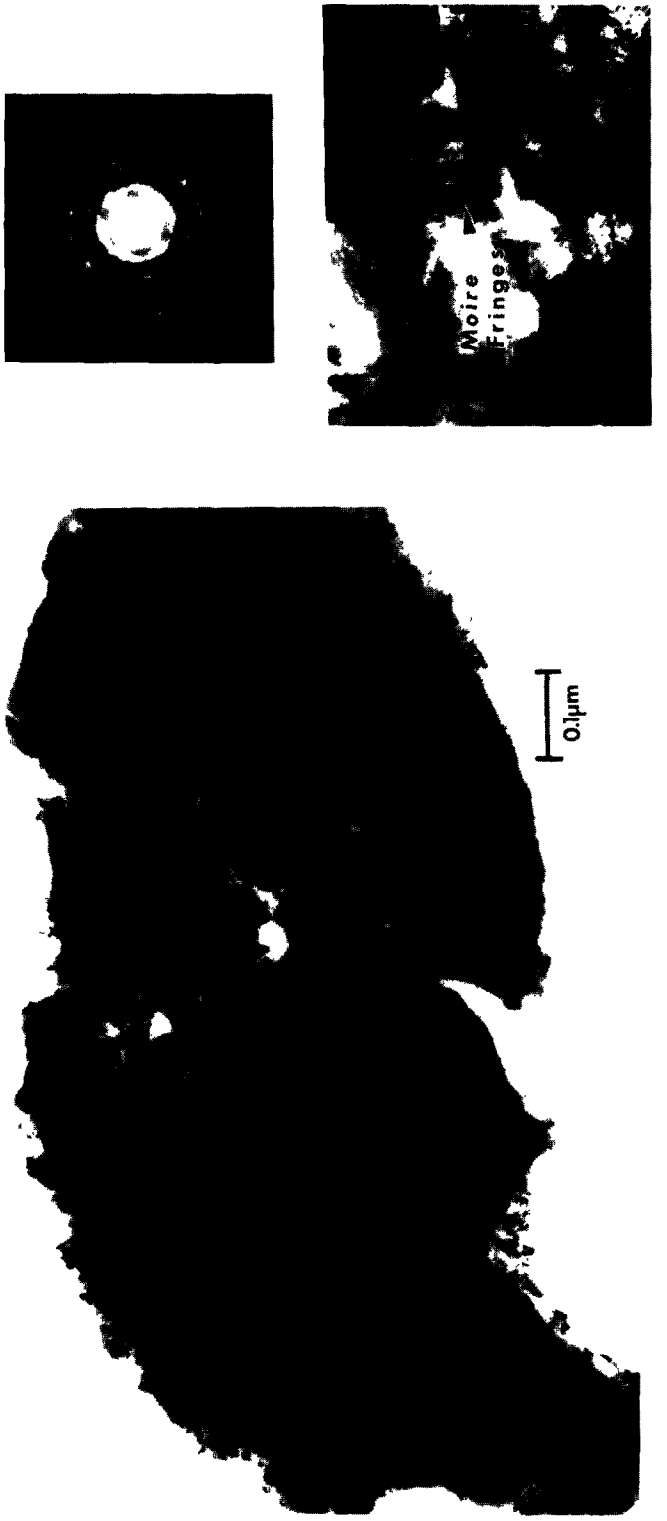

FIG. 2. Electron microscopy of Mo_2C (hcp): (a) TEM micrograph of a Mo_2C particle, (b) electron diffraction pattern, (c) magnification of a light region in panel a (3.4×).

TABLE 1

Characterization of Mo_2C (hcp)

	d-Spacings (Å) from XRD	Composition	BET surface area (m^2/g)	Irreversible CO uptake ($\mu mol/g$)	Average pore radius (Å)
After synthesis	2.61, 2.37 2.23, 1.75 1.50, 1.35	$Mo_2C_{1.04}O_{1.21}$	7.26	7.30	45.2[a]
After pretreatment	2.61, 2.37 2.23, 1.75	$Mo_2C_{0.85}O_{0.88}$	28.05	11.11	30.8[b]
After CO hydrogenation	2.61, 2.37 2.23, 1.75	$Mo_2C_{0.94}O_{0.66}$	14.93	10.00	34.1[b]
After C_2H_6 hydrogenolysis	2.61, 2.37 2.23, 1.75	$Mo_2C_{0.83}$	18.00	16.67	—

[a] From BET isotherm.
[b] From TEM.

diffraction identify the particles as the hcp phase of Mo_2C. No other bulk phases could be identified by selected area diffraction.

Elemental analysis was done on the air-exposed sample after it was evacuated at 773 K for 1 h and then transferred to a sealed vial in an Ar-purged box. Table 1 shows that the sample contains the stoichiometric amount of carbon and a very large amount of oxygen. Since neither XRD nor electron diffraction show any evidence for bulk molybdenum oxides, it is assumed that a significant fraction of the oxygen fills the octahedral voids of Mo_2C not occupied by carbon. The presence of oxygen in the Mo_2C lattice would not be detectable by XRD, since the observable peaks are due to scattering by Mo atoms. Since the measured amount of oxygen exceeds by about 20% the availability of sites in the Mo_2C lattice, it is assumed that additional oxygen may be adsorbed on the surface of the solid particles.

The location and ease of removal of oxygen from Mo_2C (hcp) were investigated by TPD and TPR (*31*). Figure 3a illustrates the TPD spectrum for an air-exposed sample. Adsorbed H_2O desorbs in two peaks centered at 400 and 575 K. The integral under these peaks corresponds to about one monolayer. Oxygen contained in the bulk of the sample is removed as CO

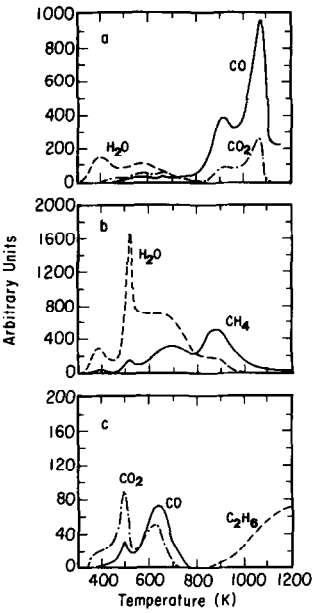

FIG. 3. TPD–TPR studies of air-exposed Mo_2C (hcp): (a) TPD spectrum of air-exposed sample, (b) TPR spectrum of an air-exposed sample, (c) additional species of observed during TPR of an air-exposed sample.

and CO_2, primarily at temperatures above 700 K. The amount of oxygen removed in these products corresponds to about 15% of the oxygen originally present in the sample. A TPR spectrum for the air-exposed sample is shown in Figs. 3b and 3c. In addition to the peaks for adsorbed H_2O, a large H_2O peak is observed at 525 K. This peak is attributable to the reduction of surface and near-surface oxygen (*31*). During TPR only small amounts of CO and CO_2 are released. The location and intensity of these peaks is identical to those observed during TPD and hence these peaks are also attributed to the removal of surface and near-surface oxygen. Figure 3b demonstrates that during TPR, a significant amount of carbon is removed as CH_4.

The results presented above clearly indicate the presence of large amounts of oxygen in Mo_2C (hcp) exposed to air. Since XRD patterns taken following reduction of MoO_3 to Mo and carburization of Mo to Mo_2C show no indications of bulk molybdenum oxides, it is concluded that the oxygen observed in the air-exposed samples is due to oxygen migration into the Mo_2C lattice. This conclusion is supported by experiments in which Mo_2C was prepared and analyzed without air exposure. Neither elemental analysis nor TPR showed any evidence of oxygen in this case. Leary *et al.* (*31*) have also demonstrated recently that Mo_2C (hcp) will take up between one and two monolayer equivalents of oxygen within minutes after air exposure and will accumulate oxygen more slowly over a period of weeks. This indicates that the rate of oxygen incorporation is significant even at room temperature, and that the incorporation of oxygen into the bulk is not due to rapid autothermal oxidation of the sample.

Prior to use of Mo_2C (hcp) for CO hydrogenation or C_2H_6 hydrogenolysis, the air-exposed catalyst was pretreated by flowing a $3/1: CH_4/H_2$ mixture at 623 K over the catalyst for 1 h and then evacuating the catalyst for 1 h. The purpose of this pretreatment was to assure carburization of any metallic Mo present on the surface and to remove as much oxygen as possible. The XRD pattern of the pretreated sample was identical to that obtained after synthesis. Elemental analysis of the pretreated sample without further air exposure revealed a 20% lowering of the carbon content and a 36% lowering in the oxygen content (see Table 1). The loss of carbon is consistent with the fact that at 75% CH_4 in the carburization mixture the CH_4/H_2 ratio is lower than that required for equilibrium (87.3%) with respect to the reaction $CH_{4(g)} \rightleftarrows C_{(s)} + H_{2(g)}$. The effectiveness of the pretreatment in removing surface oxygen is illustrated by the TPR spectrum shown in Fig. 4. The absence of any H_2O peaks below 600 K indicates that pretreatment has removed both adsorbed H_2O and oxygen from the near-surface region.

Table 1 shows that following pretreatment, the BET area and the CO uptake both increase, whereas the average pore radius decreases relative to the characteristics for the air-exposed sample following synthesis. The pattern of the changes suggests that pretreatment causes a decrepitation in the solid or removes carbonaceous matter which block the pores of the carbide. The decrease in average pore size suggests that the latter interpretation is more likely. It would also be consistent with the anticipated stoichiometry. If the sample contains 13% of the molybdenum as

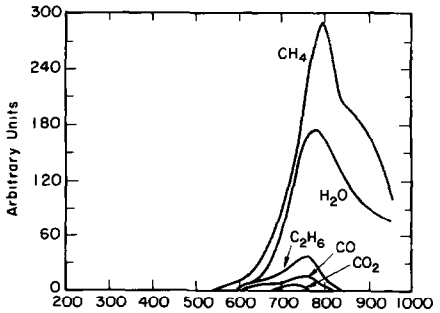

FIG. 4. Temperature-programmed reduction of pretreated Mo_2C (hcp).

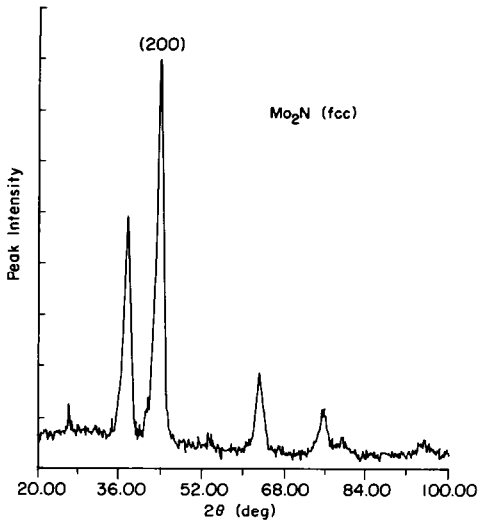

FIG. 5. XRD pattern of Mo_2N (fcc) following synthesis and air exposure.

the metal, then the stoichiometric composition should be $Mo_2C_{0.87}$, rather than Mo_2C, in good agreement with the stoichiometry observed after pretreatment. These results would then suggest that 20% of the originally present carbon is there as free carbon in the pores of the catalyst.

The pretreated catalyst was exposed to synthesis gas for 24 h at the following conditions: P_{CO} = 100 Torr, P_{H_2} = 300 Torr, and T = 573 K. The XRD pattern taken of the catalyst at the end of synthesis gas exposure was identical to that presented in Fig. 1. Elemental analysis revealed that the oxygen content had decreased by 25% and the carbon content had increased by 11% relative to that observed for the pretreated carbide. The increase in carbon content is ascribed to the deposition of free carbon in the catalyst pores during reaction. Consistent with this Table 1 shows a reduction in the BET surface area and an increase in the average pore radius. The retention of some oxygen in the sample after CO hydrogenation is attributed to the presence of H_2O in the product gases. This interpretation was confirmed by carrying out an elemental analysis on a sample of Mo_2C (hcp) which had not been air exposed prior to use for CO hydrogenation. After exposure to synthesis gas the sample showed an oxygen content similar to that seen for the air-exposed Mo_2C (hcp) sample.

A sample of pretreated Mo_2C (hcp) was also examined after 48 h of use for C_2H_6 hydrogenolysis under the following reaction conditions: $P_{C_2H_6}$ = 100 Torr; P_{H_2} = 500 Torr, and T = 573 K. Once again, XRD showed no change in the structure of the sample. The elemental analysis of the sample is given in Table 1. It is notable that following use for hydrogenolysis, the oxygen content is reduced to zero and the carbon content is consistent with that expected for a sample containing 13% metallic Mo. These results suggest that ethane hydrogenolysis at 573 K is more effective than pretreatment with a CH_4/H_2 mixture at 623 K in removing oxygen from the bulk of Mo_2C (hcp).

Mo_2N (fcc)

Freshly synthesized Mo_2N (fcc) was evacuated at 773 K for 1 h to desorb strongly adsorbed NH_3, retained from the reduction of MoO_3 with NH_3. The XRD pattern for an air-exposed sample of Mo_2N is shown in Fig. 5. The indicated d-spacings are in perfect agreement with those found previously (*33*) for Mo_2N, but the relative peak intensities are quite different. The observation of the (200) peaks as the most intense feature, rather than the (111) peak, can be ascribed to the manner of sample preparation. Volpe and Boudart (*30*) have shown that upon NH_3 reduction, the platelets of MoO_3 are converted to Mo_2N in such a way that the (200) planes of Mo_2N are exposed preferentially. The preferential orientation of the nitride particles along these planes in the sample used for XRD causes the (200) line to be emphasized.

TEM micrographs and an electron diffraction pattern for Mo_2N (fcc) are shown in Fig. 6. Since the sample is reasonably thin it could be used to identify pores by observing changes in contrast as the focal

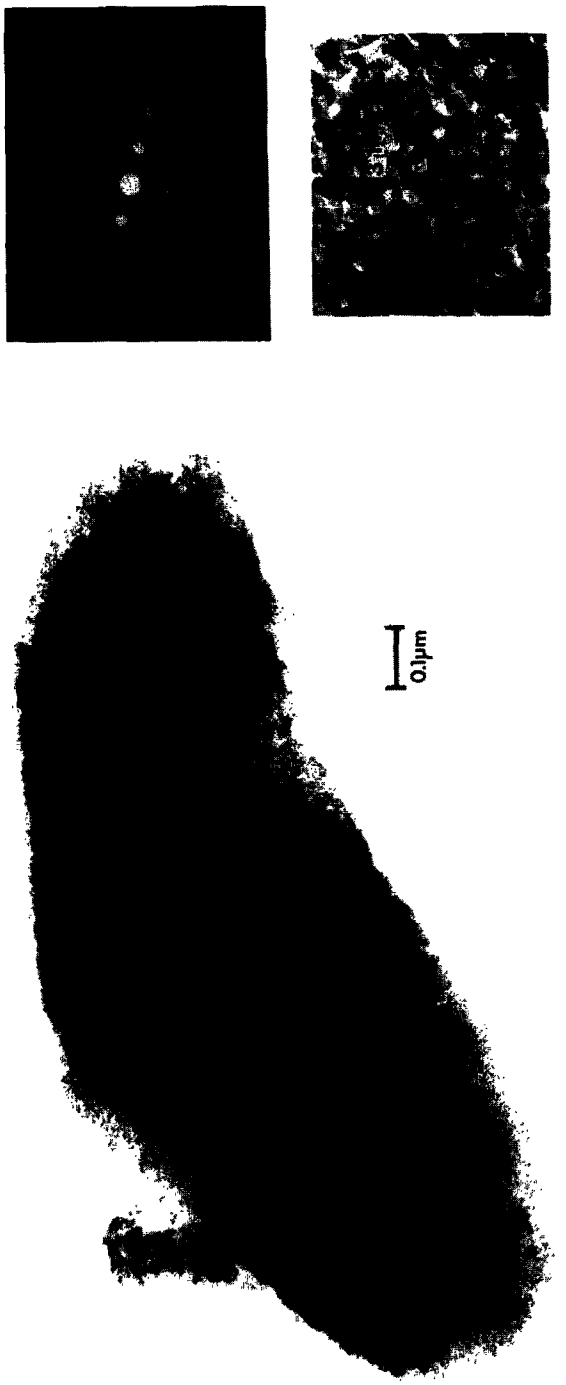

FIG. 6. Electron microscopy of Mo_2N (fcc): (a) TEM micrograph of a Mo_2N particle, (b) electron diffraction pattern of particle, (c) magnification of a light region in panel a (6.8×). Pores identified by change in contrast in a through-focus series.

TABLE 2

Characterization of Mo_2N (fcc)

	d-Spacings (Å) from XRD	Composition	BET surface area (m^2/g)	Irreversible CO uptake ($\mu mol/g$)	Average pore radius (Å)
After synthesis	2.42, 2.08 1.48, 1.27	$Mo_2N_{1.08}O_{0.19}$	185.30	559.0	17.3[a] 19.0[b]
After CO hydrogenation	2.42, 2.08 1.48, 1.27	$Mo_2N_{1.00}O_{0.51}C_{0.34}$	178.0	193.6	17.0[a]

[a] From BET isotherm.
[b] From TEM.

plane was varied. The average pore radius determined by this method is indicated in Fig. 6c and Table 2. The value agrees quite well with that determined from BET surface area and pore volume (see Table 2). The electron diffraction pattern in Fig. 6b shows well-defined spots indicative of a highly crystalline sample and in good agreement with the observations of Volpe and Boudart (*30*). The diffraction pattern is characteristic of (200) and (100) planes of Mo_2N.

The results of elemental analysis are given in Table 2. The sample contains the stoichiometric amount of nitrogen and a small amount of oxygen. The latter element is residual from the MoO_3 since the sample was not air exposed prior to analysis.

The BET surface area and CO uptake capacities of Mo_2N (fcc) are given in Table 2. Of the total CO taken up, 56% is held irreversibly. These results are in good agreement with those reported by Volpe and Boudart (*30*) and are indicative of our ability to reproduce their preparation of high-surface area Mo_2N. A further characteristic worth noting is that the chemisorption capacity of the sample for NH_3 is virtually the same as that for CO. Since it is known (*35*) that NH_3 bonds to Mo atoms at on top sites, it may be inferred that CO adsorbs in similar sites.

Following synthesis and evacuation for 1 h at 773 K, a sample of Mo_2N (fcc) was exposed to synthesis gas at the same conditions used for Mo_2C (hcp). The XRD pattern use of the catalyst was identical to that shown in Fig. 5. Elemental analysis (see Table 2) showed no loss of nitrogen but a definite increase in the oxygen content and the accumulation of some carbon. The extent to which the carbon enters the lattice was not determined. The significant reduction in CO uptake capacity following CO hydrogenation suggests that a part of the carbon inventory may be present as free carbon on the catalyst surface. Pore blockage by carbon does not seem to occur since neither the BET surface area nor the average pore radius is altered significantly.

Mo_2C (fcc)

The synthesis of Mo_2C (fcc) according to the procedures described in the Experimental section produced a material which analyzed as 8.5 wt% carbon and had little capacity for CO chemisorption. Since the stoichiometric amount of carbon is 5.9 wt%, it was concluded that the excess carbon was present on the surface of the freshly prepared Mo_2C (fcc). The amount of excess carbon could be reduced and the CO chemisorption capacity increased by air exposure of the sample, and consequently, this procedure was adopted. Table 3 indicates that following air exposure the sample still contains an excess of carbon and a very large amount of oxygen.

TABLE 3

Characterization of Mo_2C (fcc)

	d-Spacings (Å) from XRD	Composition	BET surface area (m^2/g)	Irreversible CO uptake (μmol/g)	Average pore radius (Å)
After synthesis	2.44, 2.11 1.49, 1.28	$Mo_2C_{1.29}O_{2.07}$	140.0	340.0	13.7[a] 13.5[b]
After pretreatment	2.44, 2.11 1.49, 1.28	$Mo_2C_{1.13}O_{3.03}$	139.3	62.3	20.6[a]
After CO hydrogenation	2.44, 2.22 1.49, 1.28	$Mo_2C_{0.99}O_{0.73}$	122.0	110.0	—
After C_2H_6 hydrogenolysis	2.44, 2.11 1.49, 1.28	$Mo_2C_{0.89}O_{0.69}$	161.0	140.0	—

[a] From BET isotherm.
[b] From TEM.

The XRD pattern of air-exposed Mo_2C (fcc) is shown in Fig. 7. The indicated *d*-spacings are somewhat larger than those reported in the literature for fcc phase of oxygen-free Mo_2C (*33*), and consistent with this the lattice constant for our sample is 4.225 Å instead of the expected 4.14 Å. The larger lattice constant is suggestive of a large content of nonmetal in the host fcc lattice of Mo. For example, Ferguson (*36*) has reported a lattice constant of 4.152 for $Mo_2C_{0.6}O_{0.8}$ and Rudy (*37*) has reported lattice constants ranging from 4.226 to 4.281 Å for molybdenum carbides with stoichiometries ranging between $Mo_2C_{1.38}$ and $Mo_2C_{1.5}$. It should be noted that the XRD pattern presented in Fig. 7 shows no evidence for metallic molybdenum or molybdenum oxides.

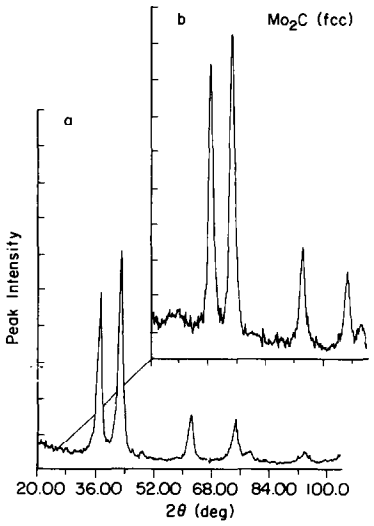

FIG. 7. XRD patterns of Mo_2C (fcc): (a) following synthesis and air exposure, (b) following CO hydrogenation and air exposure.

Additional structural information was obtained from TEM studies. TEM micrographs and an electron diffraction pattern are shown in Fig. 8. The electron diffraction pattern shows well-defined spots indicative of a highly crystalline lattice and the spacing of the spots is characteristic of a Mo_2C (fcc) lattice. Contrast variation observed upon variation of the focal plane was used to identify pores in the sample, and pores between 3 and 30 Å were observed. As indicated in Table 3, the agreement in average pore radius determined from TEM micrographs and BET isotherms is very good.

Mo_2C (fcc) was pretreated in a CH_4/H_2 mixture prior to CO hydrogenation. As seen in Table 3, the most dramatic change is the large increase in oxygen content relative to that for the catalyst after synthe-

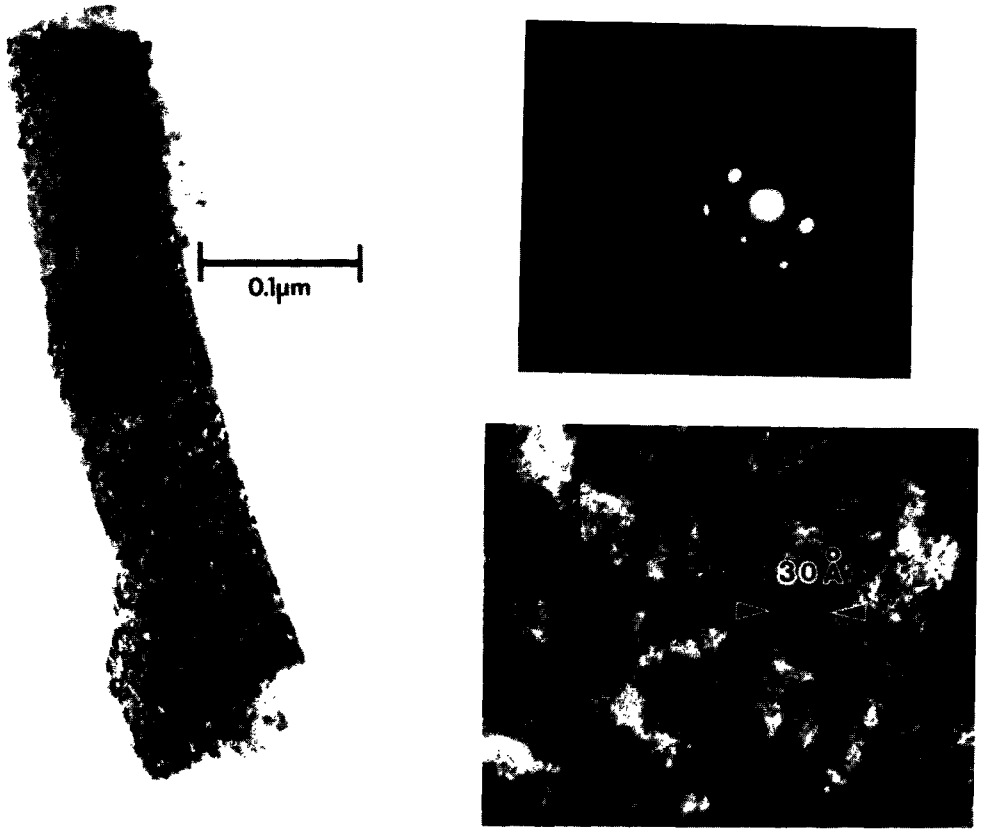

FIG. 8. Electron microscopy of Mo_2C (fcc): (a) TEM micrograph of a Mo_2C particle, (b) electron diffraction pattern of particle, (c) magnification of a light region in panel a (4.1×). Pores identified by change in contrast in a through-focus series.

sis. On the other hand, the carbon content decreased slightly as a result of pretreatment. It is suspected that the high oxygen content results from a slow accumulation of oxygen or water during its storage after pretreatment. XRD, however, showed no evidence of molybdenum oxides, indicating that the oxygen must be stored in the carbide lattice or on the surface of the carbide particles.

The pretreatment of Mo_2C (fcc) was successful in removing surface oxygen. The TPR spectrum presented in Fig. 9 shows no water formation below 600 K. While not shown, TPR spectra of air-exposed Mo_2C (fcc) show peaks for H_2O, CO, and CO_2 at temperatures below 600 K, much as was seen in Fig. 4 for Mo_2C (hcp). The absence of these features following pretreatment is indicative of the removal of adsorbed H_2O and near-surface oxygen from the sample.

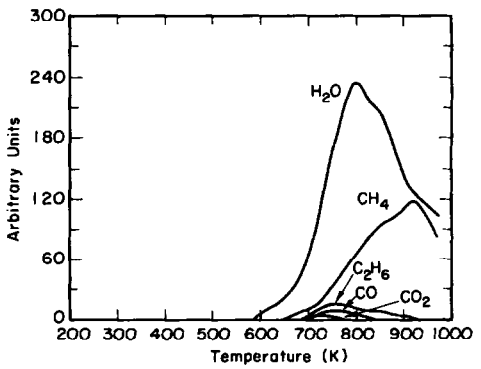

FIG. 9. Temperature-programmed reduction of pretreated Mo_2C (fcc).

Following pretreatment, a sample of Mo_2C (fcc) was used for CO hydrogenation under the same conditions used for Mo_2C (hcp) and Mo_2N (fcc). The XRD pattern of the used catalyst was identical to that shown in Fig. 7. As shown in Table 3, elemental analysis revealed a reduction in the carbon content down to the stoichiometric level and a very significant reduction in the oxygen content. Consistent with the removal of excess carbon, the capacity for CO adsorption is found to increase significantly. The small decrease in BET surface area observed in this case is ascribed to structural changes in the carbide rather than pore blockage by carbon. The loss of oxygen from the catalyst during CO hydrogenation is supported by the TPR spectrum shown in Fig. 10. Notice that in contrast to the TPR spectrum of the pretreated catalyst, Fig. 9, the production of water does not occur below 900 K and the amount produced is much less. The absence of H_2O for temperatures below 600 K again indicates that the near-surface region of the catalyst is free of oxygen.

Ethane hydrogenolysis was carried out over pretreated Mo_2C (fcc) using the same reaction conditions used for Mo_2C (hcp). XRD again failed to show any change in the catalyst structure. Changes could, however, be detected by other techniques. As seen in Table 3, the carbon and oxygen contents of the carbide are lower than those observed following pretreatment. The increase in BET surface area and CO adsorption capacity both suggest that the hydrogenolysis of ethane leads to a removal of excess carbon from the catalyst surface and pores. Comparison of the responses of Mo_2C (hcp) and Mo_2C (fcc) to ethane hydrogenolysis indicates that while hydrogenolysis causes a strong reduction in the oxygen content of both carbides, the complete removal of oxygen from the fcc structure is not achieved even after 48 h of reaction.

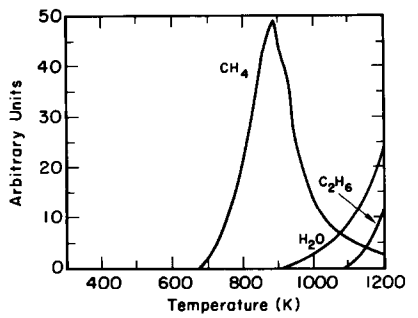

FIG. 10. Temperature-programmed reduction of Mo_2C (fcc) following CO hydrogenation.

DISCUSSION

In the preparation of molybdenum carbides it is difficult to avoid the deposition of free carbon, particularly if complete conversion of Mo to Mo_2C is sought. For the conditions used in the present study the stoichiometry of the C/Mo ratio of the freshly prepared Mo_2C (hcp) is 0.52. Since XRD shows that only 87% of the Mo is present as Mo_2C this means that the sample has about 9.0 wt% of free carbon. A similar analysis for Mo_2C (fcc) indicates that the freshly prepared sample (prior to air exposure) has 3.6 wt% of free carbon. While the elimination of excess carbon by H_2 reduction has been recommended by several authors (*11, 13, 21, 30*), Leary *et al.* (*31*) have shown recently that even at 623 K it is not possible to do this without removing significant amounts of bulk carbon concurrently.

When either the hcp or fcc form of Mo_2C is air exposed, oxygen is rapidly incorporated into the lattice. Attempts to passivate high-surface area Mo_2C (fcc) with a 1% O_2 in He mixture, as recommended by Boudart and Volpe (*30*) were unsuccessful, inasmuch as additional oxygen uptake continued after the sample was exposed to air at room temperature. If the initial exposure to oxygen is carried out without elevation in the sample temperature, oxygen will incorporate into the lattice without a corresponding loss of carbon. Prolonged (~1 month) air exposure, even at room temper-

ature leads to a progressive loss of carbon from the carbide. It is significant to note that the presence of oxygen in the carbide cannot be detected by X-ray or electron diffraction since these techniques are sensitive primarily to the Mo lattice and the lattice parameters change only slightly with changes in the O/C ratio in the lattice. Consequently, it is essential to perform careful elemental analyses of molybdenum carbides in order to determine their oxygen content.

Leary *et al.* (*31*) have shown that lattice oxygen cannot be removed from $Mo_2C_xO_y$ by H_2 reduction without simultaneous removal of lattice carbon. This conclusion is also strongly supported by the TPR results presented in Figs. 3b and 3c. The TPR spectrum presented in Fig. 4 does show, however, that near-surface oxygen can be removed from the air-exposed Mo_2C by pretreatment with a CH_4/H_2 mixture at 623 K.

The present study also demonstrates clearly that the bulk composition of molybdenum carbide and nitride catalysts is influenced strongly by the reaction conditions under which these catalysts are used. For example, air-exposed Mo_2C (hcp) or Mo_2C (fcc) will rapidly incorporate oxygen, while air-exposed samples of these same catalysts will lose oxygen during CO hydrogenation. The deposition or removal of free carbon can also occur during this reaction as shown by the results presented in Tables 1–3. The hydrogenolysis of C_2H_6 also influences catalyst composition. As seen in Tables 1 and 3, this reaction is particularly effective in removing lattice oxygen from molybdenum carbides, in good agreement the earlier observations of Leclerq *et al.* (*11*). A discussion of the effects of catalyst composition on the activities of Mo_2C and Mo_2N for CO hydrogenation and hydrogenolysis will be presented separately (*32*).

Since the chemisorption of CO is often used to characterize the surface of molybdenum carbides and nitrides, it is of interest to compare the uptakes reported here with those given in earlier studies. Madix and Ko (*7*) have carefully examined the chemisorption of CO on a fully carburized surface of Mo(100). The carbon atoms sit in fourfold hollows on the metal surface, forming a (1 × 1)C overlayer. The structure of the fully carburized Mo(100) surface resembles that of the (200) surface of Mo_2C (fcc). CO adsorption occurs on top of the exposed Mo atoms and the saturation coverage is found to be 1×10^{15} molecules/cm^2. This value agrees quite well with those calculated for the (101) surface of Mo_2C (hcp) [0.6×10^{15} molecules/cm^2] and the (200) surface of Mo_2C (fcc) [1.17×10^{15} molecules/cm^2]. Since the structure of Mo_2N (fcc) is virtually identical to that of Mo_2C (fcc), the saturation uptake of CO would be expected to be the same.

Table 4 lists the saturation-level surface concentrations of adsorbed CO determined in this study, as well as those of Boudart and co-workers (*11, 13, 30*). In each case, the surface concentration was obtained by dividing the CO uptake by the BET surface area. It is evident that the surface concentrations of adsorbed CO found in this study for molybdenum oxycarbides are in general agreement with the values reported earlier by Leclerq *et al.* (*11*) but are significantly lower than those reported by Boudart and Volpe (*30*). On the other hand, the saturation concentration for Mo_2N (fcc) found here and that reported by Boudart and Volpe (*30*) are in reasonable agreement. It is significant to note, though, that all the values given in Table 4 are smaller than those expected for single crystal surfaces of Mo_2C or Mo_2N.

The surface of freshly prepared Mo_2N retains a significant amount of adsorbed NH_3, left over from the reduction of MoO_3 in NH_3. If adequate care is not exercised to remove all of the residual NH_3, then sites for CO adsorption will be blocked by NH_3. This might explain why the CO saturation concentrations measured for high surface area Mo_2N (fcc) (see Table 4) powders is lower than that expected for clean crystal

TABLE 4

CO Chemisorption Capacity

Catalyst	CO capacity × 10^{-14} (molecules/cm^2)				
	After synthesis	After pretreatment	After CO hydrogenation	After C_2H_6 hydrogenolysis	Ref.
Mo_2 (hcp)	0.60	0.24[a]	0.40	0.56	This work
Mo_2C (hcp)	3.00	—	—	—	(*12*)
Mo_2C (hcp)	—	0.18[b]	—	—	(*13*)
Mo_2C (fcc)	1.46	0.27[a]	0.54	0.52	This work
Mo_2C (fcc)	—	0.40[b]	0.23	—	(*11*)
Mo_2C (fcc)	—	—	0.63[c]	—	(*11*)
Mo_2C (fcc)	—	3.09[d]	—	—	(*30*)
Mo_2N (fcc)	1.18	—	0.65	—	This work
Mo_2N (fcc)	2.60	—	—	—	(*30*)

[a] Heated in 3/1 : CH_4/H_2 mixture at 623 K for 1 h.

[b] Heated in H_2 at 623 K for 2 h and then evacuated at 623 K for 2 h.

[c] Heated in a 9.1 : C_4H_{10}/H_2 mixture at 773 K for 3 h prior to exposure to synthesis gas.

[d] Heated in H_2 at 870 K for 2 h.

surfaces. The low CO surface concentrations for Mo_2C reported by Leclerq *et al.* (*11*) and ourselves is very likely due to surface blockage by free carbon. This argument is consistent with the fact that carbon accumulation on the surface of Mo_2N (following CO hydrogenation) causes a suppression in the concentration of adsorbed CO at saturation. In the work of Volpe and Boudart (*30*) efforts were made to rid the surface of Mo_2C (fcc) of free carbon. This was done by reducing the sample at 870 K in H_2 for 2 h. Whereas Table 4 shows that such pretreatment does lead to a CO surface concentration higher than that observed on samples containing free carbon, the high temperature at which reduction was carried out may have removed a significant amount of carbon from the bulk of the sample. Consequently, we believe that the reduced samples of Mo_2C (fcc) described by Volpe and Boudart (*30*) very likely consisted of a layer of metallic Mo over a core of Mo_2C. This might explain why they observed such high CO surface concentrations.

CONCLUSIONS

Porous powders of Mo_2C (hcp), Mo_2C (fcc), and Mo_2N (fcc) have been prepared from MoO_3. Mo_2C (hcp) was prepared by H_2 reduction of MoO_3 to metallic Mo and subsequent carburization in a mixture of CH_4 and H_2. The product is a polycrystalline powder which has a BET surface area of 10–30 m^2/g and pores 30 Å in diameter. Mo_2N (fcc) was obtained by NH_3 reduction of MoO_3. The nitride is highly crystalline, has a BET surface area of 180 m^2/g, and pores 17 Å in diameter. The fcc phase of Mo_2C was produced by heating Mo_2N (fcc) in a mixture of CH_4 and H_2. The Mo_2C (fcc) powder has a BET surface area of 140 m^2/g and pores 21 Å in diameter.

In the preparation of the hcp and fcc phases of Mo_2C it is very difficult to avoid the deposition of free carbon, particularly when complete conversion of Mo to the carbide is sought. The presence of free carbon reduces the CO chemisorption capacity of the carbide, and at higher levels of accumulation blocks the pores in the car-

bide. Removal of free carbon by high temperature H_2 reduction cannot be accomplished without significant removal of bulk carbon. Air exposure of Mo_2C will remove some of the free carbon but introduces O into the carbide lattice. Passivation of Mo_2C samples to oxygen accumulation is not possible. The presence of oxygen in air-exposed samples of Mo_2C cannot be detected by XRD, since this technique is sensitive primarily to the location of the Mo atoms and not to the position of the nonmetal atoms. Consequently, the oxygen content of molybdenum oxycarbides must be determined by elemental analysis. Lattice oxygen cannot be removed by H_2 reduction without a concurrent removal of lattice carbon. Near-surface oxygen can be eliminated by thermal pretreatment in a CH_4/H_2 mixture. This procedure does, however, remove some of the carbon from the near-surface region.

The composition of Mo_2C and Mo_2N is altered by their use for CO hydrogenation and C_2H_6 hydrogenolysis. CO hydrogenation releases carbon and oxygen. The carbon accumulates on the catalyst surface, whereas the oxygen enters into the lattice of Mo_2C or Mo_2N. By contrast, C_2H_6 hydrogenolysis results in extensive removal of oxygen from the lattice of the hcp and fcc modifications of Mo_2C. This process is unaccompanied by the deposition of free carbon, very likely because the presence of H_2 in the reaction mixture removes any surface carbon as methane.

ACKNOWLEDGMENTS

The authors thank Mr. K. Leary for his assistance in acquiring TPD and TPR spectra and Dr. M. L. Sattler for her assistance in taking electron micrographs of Mo_2C and Mo_2N. This work was supported by the Office of Basic Energy Sciences, Material Sciences Division of the U.S. Department of Energy, under Contract DE-AC03-76SF00098.

REFERENCES

1. Storms, E. K., "The Refractory Carbides." Academic Press, New York, 1967.
2. Toth, L. E., "Transition Metal Carbides and Nitrides." Academic Press, New York, 1971.
3. V. Heine, *Phys. Rev.* **153,** 673 (1967).
4. Siegel, E., *Semicond. Insul.* **5,** 47 (1979).
5. Williams, A. R., Gelatt, C. D., Connolloy, J. W. D., and Moruzzi, V. L., "Mater. Res. Soc. Symp. Proc.," Vol. 19, p. 17. Elsevier, New York, 1983.
6. Ko, E. I., and Maddix, R. J., *Surf. Sci.* **100,** L449, L505 (1980).
7. Ko, E. I., and Maddix, R. J., *Surf. Sci.* **109,** 221 (1981).
8. Levy, R. B., *in* "Advanced Materials in Catalysis" (J. J. Burton and R. L. Garten, Eds.). Academic Press, New York, 1977.
9. Oyama, S. T., and Haller, G. L., *in* "Catalysis" (G. C. Bond and G. Webb, Eds.), Specialist Periodical Reports, Vol. 5, p. 333. The Chemical Society, London, 1981.
10. Leclerq, L., *in* "Surface Properties and Catalysis by Non-Metals" (J. P. Bonnelle, Ed.), p. 433. Reidel, New York, 1983.
11. Leclerq, L., Imura, K., Yoshida, S., Barbee, T., and Boudart, M., *in* "Preparation of Catalysts II" (B. Delmon, Ed.), p. 627. Elsevier, New York, 1978.
12. Saito, M., and Anderson, R. B., *J. Catal.* **63,** 438 (1980).
13. Boudart, M., Oyama, S. T., and Leclerq, L., *in* "Proceedings, 7th International Congress on Catalysis, Tokyo, 1980" (T. Seiyama and K. Tanabe, Eds.), p. 578. Elsevier, Amsterdam, 1981.
14. Slaugh, L. H., and Hoxmeier, R. J., U.S. Patent No. 4,326,992, April 27, 1982.
15. McCandlish, L. E., Wright, F. J., and Kugler, E. L., U.S. Patent No. 4,345,038, August 17, 1982.
16. Bridgewater, A. J., Burch, R., and Mitchell, P. C. H., *J. Catal.* **78,** 116 (1982).
17. Murchison, C. B., *in* "Fourth Inter. Conf. on Chem. and Uses of Mo" (H. Barry, Ed.), p. 197. Climax Molybdenum Co., Ann Arbor, MI, 1982.
18. Dun, J. W., Gulari, E., and Ng, K. Y. S., *Appl. Catal.* **15,** 247 (1985).
19. Shigehara, Y., *Nippon Kagaku Kaishi* **4,** 474 (1977).
20. Shigehara, Y., *Nippon Kagaku Kaishi* **10,** 1438 (1977).
21. Kojima, I., Miyazaki, E., Inoue, Y., and Yasumori, I., *J. Catal.* **59,** 472 (1979).
22. Kojima, I., Miyazaki, E., and Yasumori, I., *J. Chem. Soc. Comm.*, 573 (1980).
23. Kojima, I., Miyazaki, E., Inoue, Y., and Yasumori, I., *J. Catal.* **73,** 128 (1982).
24. Levy, R. B., and Boudart, M., *Science* **181,** 547 (1973).
25. Burch, R., and Mitchell, P. C. H., *J. Less-Common Metals* **54,** 363 (1977).
26. Bridgewater, A. J., Burch, R., and Mitchell, P. C.

H., *J. Chem. Soc. Faraday Trans. I* **76,** 1811 (1980).
27. Mittasch, A., "Advances in Catalysis and Related Subjects," Vol. 2, p. 81 (1950).
28. Yang, R. T., and Wong, C., *J. Catal.* **85,** 154 (1984).
29. Tsuchimoto, K., Suzuki, M., and Yamaki, N., *Nippon Kagaku Kaishi* **10,** 1420 (1979).
30. Volpe, L., and Boudart, M., *J. Solid State Chem.* **59,** 332, 348 (1985).
31. Leary, K. J., Michaels, J. N., and Stacy, A. M., *J. Catal.* **101,** 301 (1986).
32. Ranhotra, G. S., Bell, A. T., and Reimer, J. A., *J. Catal.* **108,** 40 (1987).
33. Melune, W. F. (Ed.), "JCPDS 1980 Powder Diffraction File-Inorganic." Univ. of Pennsylvania, Philadelphia, 1980.
34. Thomas, G., and Govinge, M. J., "Transmission Electron Microscopy." Wiley, New York, 1979.
35. Haddix, G., Reimer, J. A., and Bell, A. T., unpublished results.
36. Ferguson, I. F., Ainscough, J. B., Morse, D., and Miller, A. W., *Nature (London)* **202,** 1327 (1964).
37. Rudy, E., AFML-TR-65-2, Part 1, Vol. II, Air Force Materials Laboratory, Wright Patterson Air Force Base, OH, 1965.